
Fundusze Europejskie dla Nowoczesnej Gospodarki
Rzeczpospolita Polska
Dofinansowane przez Unię Europejską
PARP Grupa PFR
Fiber-Optic Seismograph performance investigation during artificial explosions at the field test performed at the Szopowe, Poland
https://fosrem.eu
ELPROMA
Anna Kurzych[1,2], Leszek R. Jaroszewicz[1,2], Michał Dudek[1,2], Paweł Zinówko[2], Karol Konarski[2]
[1]Institute of Applied Physics, Military University of Technology, 2 gen. S. Kaliskiego Str., 00-908 Warsaw, Poland
[2]Elproma Electronics Ltd., 2A Duńska Str., 05-152 Czosnów, Poland
AIS 2024
The 1st International Conference on AI Sensors
and
The 10th International Symposium on Sensor Science
1-4 August 2024, Singapore
I3S 2024

Motivation

01 Rotational Seismology

a new, emerging field for the study of all aspects of rotational ground motion induced by earthquakes, explosions, and ambient vibrations [Lee et al. *BSSA*, **99**, (2009) 945-957]

02 Engineering application

seismic behaviour of irregular and complex civil structures [Trifunac, *BSSA*, **99**, (2009), 968-97; Mustafa, InTech, 2015]

03 Seismological application

broadband seismology [Igel et al., *Geophys. J. Int.*, **168**(1), (2006), 182–197], **strong-motion seismology** [Anderson, 2003, Chap. 57, 937-965], **earthquake physics** [Teisseyre et al. Springer, 2006; Springer, 2008], **seismic hazards** [McGuire, *Earthq. Eng. Struct. D.*, **37**, (2008), 329–338], **seismotectonic's** [www.geophysik.un-muenchen.de/~igel/Lectures/Sedi/ sedi_tecto nics.ppt], **geodesy** [Carey, Expanding Earth Symposium, (1983), 365-372], **physicists using Earth-based observatories for detecting gravitational waves** [Ju] et al., *Rep. Prog. Phys.*, **63**, (2000), 1317–1427; Lantz et al., *BSSA*, **99**, (2009), 980-989

04 6-DoF

earthquake sources, tilt correction, wavefield separation, wave direction, wave dispersion, scattering properties, seismic imaging [Murray-Bergquist et al. Sensors, 21 (2021), 3732]

[https://www.britannica.com/list/7-women-warriors]

[https://www.businessinsider.com/earthquake-taiwan-east-coast-2018-2?IR=T]

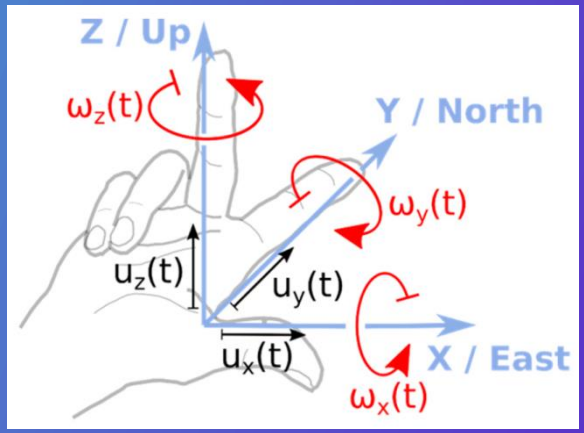

Tombstone in Kushiro Cemetery after the Tokachi-Oki Earthquake 2003 [Hinzen, J. Seismol., 16(4), (2012), 797–814]

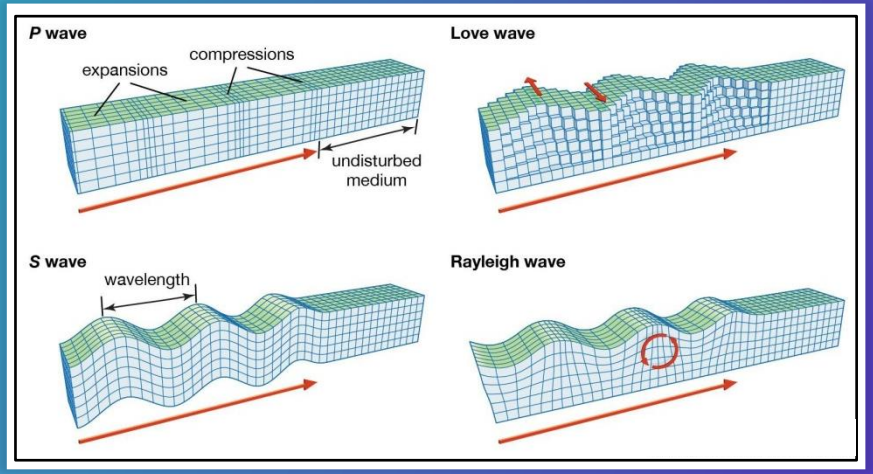

[https://geologyscience.com/natural-hazards/earthquakes/seismic-waves/]

Seismological application

Energy generated during an earthquake propagates not only in a form of linear motions but also in rotational ones. Earthquakes are undoubtedly one of the most complex phenomena and it is hard to entirely reflect their complexity in theoretical models

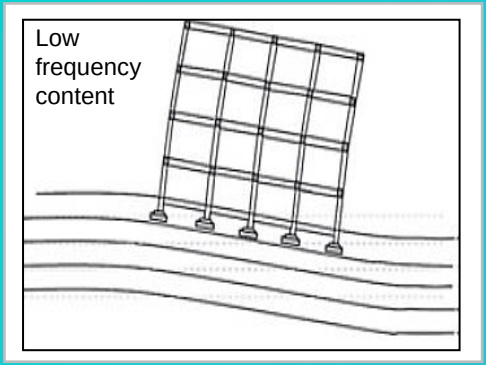

- Higher stress in structural element
- **Overturning moment**
- Horizontal displacement of the center of mass

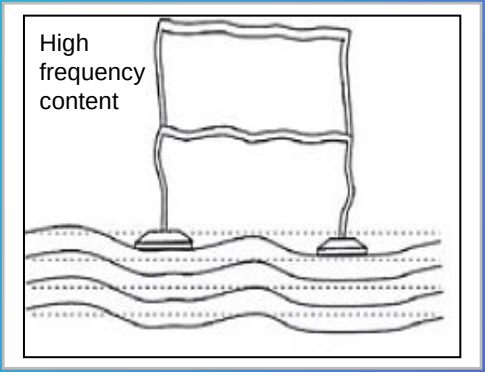

- **Local vibration of beams and columns**
- Meaningless motion of the building center of mass

[Castellani, Guidotti, 2nd Workshop of IWGoRS Masaryk 's College Prague, (2010)]

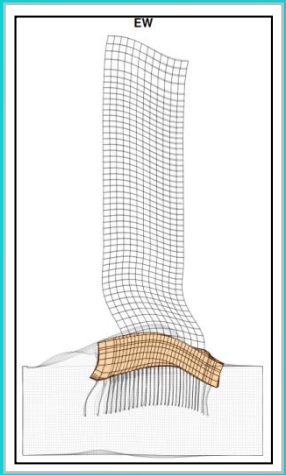

Snapshot of the model of displacement response to an incident plane P-wave half sine displacement pulse with 45° incident angle (view from South) [Todorovska M. I., WCEE2024 Processing, 2024]

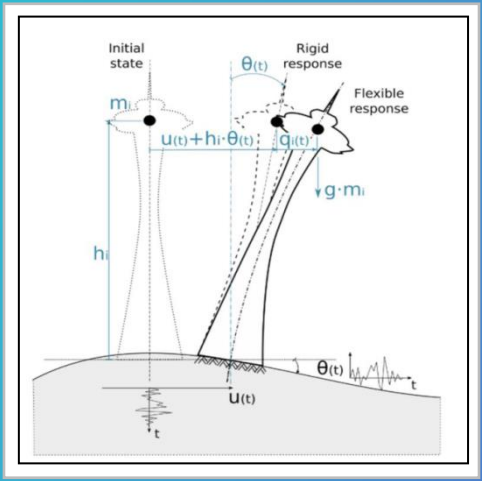

A slender structure under horizontal-rocking ground vibrations [Bońkowski et al., Engineering Structures 155, 387–393, 2018]

Engineering application

For tall structures, even a tiny rocking motion of the building foundation may matter

Requirements

Engineering application

signal amplitude: up to 10 rad/s,
frequency: 0.01 Hz – 100 Hz

Seismological application

signal amplitude: from 10^{-11} rad/s,
frequency: 0.01 Hz – 0.1 Hz

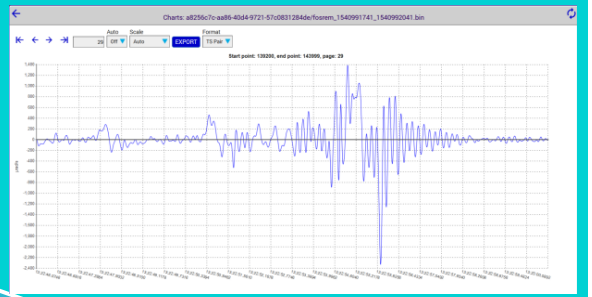

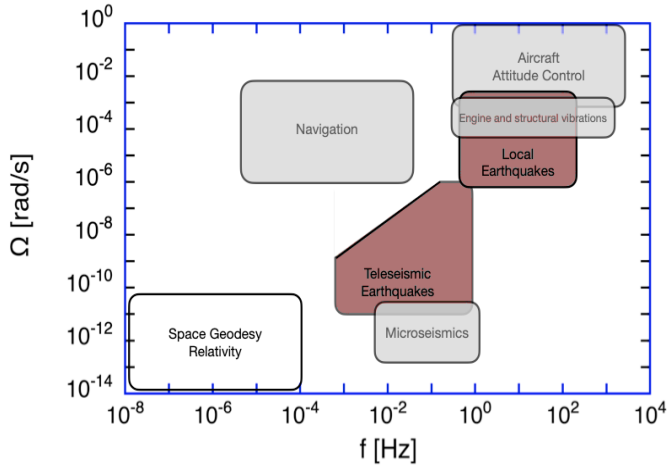

[Schreiber U, Kodet J, WCEE Processing, Milan, Italy 2024]

- Insensitivity to linear motion
- Mobility, stability with respect to environmental conditions, including changes of temperature
- Independent power supply
- Dynamic range 10^{-8} - 10 rad/s
- Frequency band 0.01 - 100 Hz
- Power consumption 5 – 8 W
- Thermal stability <0,1% / °C
- Calibration – in situ (permanently)

ROTATIONAL SEISMOGRAPH
network of seismometers + precise time source + recording device + network

[Bernauer et al., J. Seismol., 16, (2012)] [Jarozsewicz et al., Sensors, 16, 2161 (2016)]

BACKGROUND

The direct utilization of the Sagnac effect

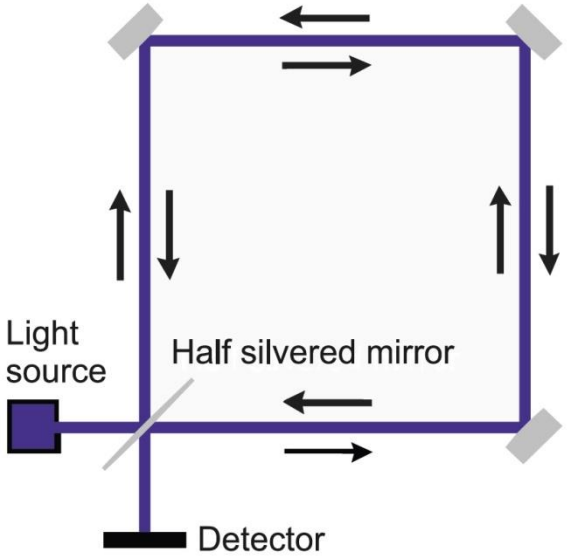

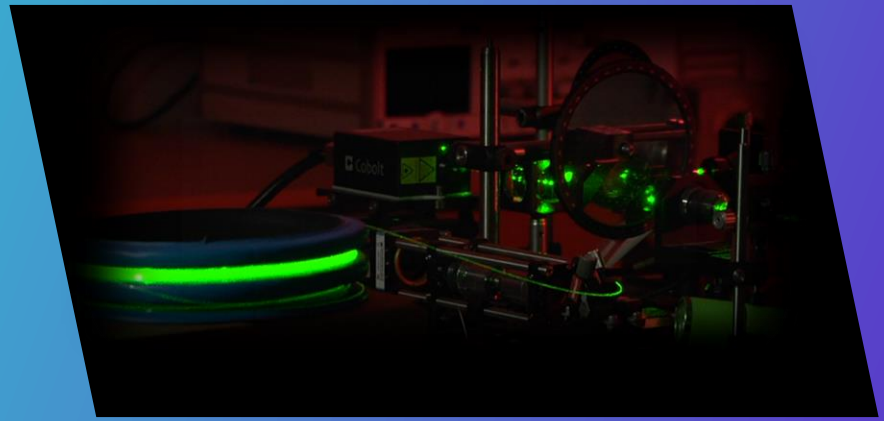

Sagnac effect (1913) shows the difference between phase of two beams propagating around closed optical path, in opposite direction when this path is rotating with rotational rate Ω.

In a fibre-optic implementation (1978) the rotation rate Ω is expressed by induced phase shift Δφ as:

$$\Omega = S_o \cdot \Delta\varphi = \frac{\lambda c}{4\pi RL} \cdot \Delta\varphi$$

L – length of the fiber in the sensor loop, R – sensor loop radius, λ – wavelength of used source, c – velocity of the light in vacuum, S_0 – the optical constant of an interferometer

Fibre-Optic Rotational Seismograph

historical brief

1998

GS-13P
Ω_{min}: $3.49 \cdot 10^{-3}$ rad/s
SL: 380 m PANDA
Radius: 0.1 m

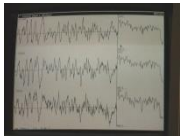

2001

FORS-I
Ω_{min}: $2.2 \cdot 10^{-6}$ rad/s
Ω_{max}: $4.8 \cdot 10^{-4}$ rad/s
SL: 400 m PANDA
Radius: 0.1 m

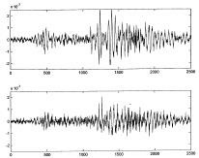

2010

FORS-II, FOS1
Ω_{min}: $4.2 \cdot 10^{-8}$ rad/s
Ω_{max}: $4.8 \cdot 10^{-4}$ rad/s;
SL: 11 000 m SMF
Radius: 0.34 m
FOS2
Ω_{min}: $4 \cdot 10^{-9}$ rad/s,
Ω_{max}: $6.4 \cdot 10^{-3}$ rad/s
SL: 15 000 m SMF
Radius: 0.34 m

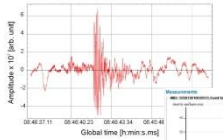

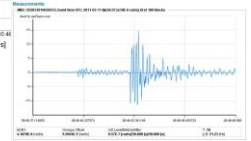

2015

FOSREM – FOS3 & FOS4
Ω_{min}: $2 \cdot 10^{-8}$ rad/s,
Ω_{max}: few rad/s
SL: 5 000 m SMF
Radius: 0.125 m

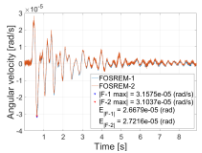

2018

FOS5
Ω_{min}: $7 \cdot 10^{-8}$ rad/s,
Ω_{max}: 10 rad/s
SL: 5 000 m SMF,
Radius: 0.125 m

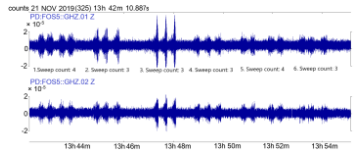

2023

FOS6
3- Axis with 100 ns time synchronization
Ω_{min}: several dozen nrad/s
Ω_{max}: 10 rad/s
SL: 6 000 m SMF
Radius: 0.125 m
Weight: 10 kg

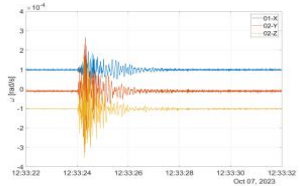

Fibre-Optic Seismograph

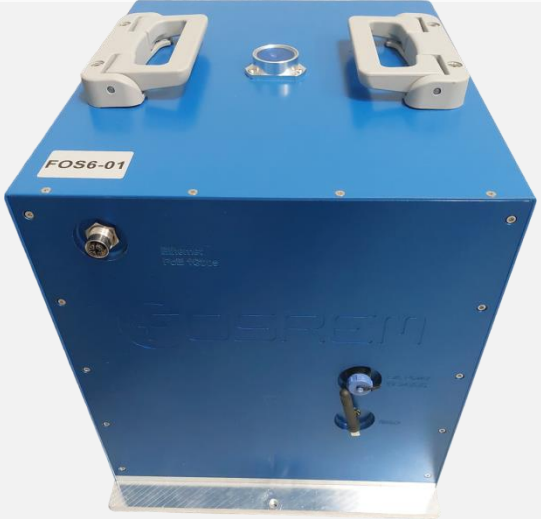

OPTICAL PART

generates the phase shift $\Delta\varphi$ proportional to the measured rotation rate Ω which is perpendicular to the sensor loop plane

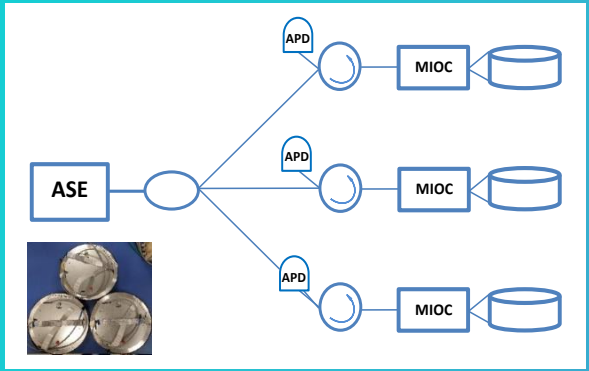

ELECTRONIC PART

enables to calculate and record information about rotational motions via digital closed-loop signal processing

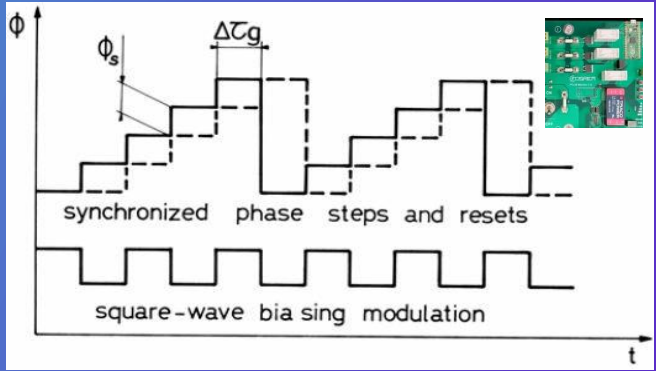

Laboratory analysis of FORS' parameters

Allan Variance analysis
Theoretically

$$S = \frac{\sqrt{2}\lambda c}{2\pi DL}\sqrt{\frac{4kT}{R\eta^2P^2} + \frac{ei_d}{\eta^2P^2} + \frac{e}{\eta P} + \frac{\lambda^2}{4c\Delta\lambda}} \equiv_{|\Delta B=1Hz} \text{ ARW}$$

where: λ – central light wavelength (1 550 nm), c – speed of light, D – loop diameter (0.25 m), L – loop length (about 6 000 m), k – Boltzmann's constant, T – temperature (293 K), R – resistance of the trans-impedance transducer of the photodetector device (20 kΩ), η – efficiency ratio of the photodiode (0.85 A/W), P – incident optical power on the APD, e – elementary charge, i_d – photodiode dark current (80 nA), $\Delta\lambda$ – spectral width of the light source (40 nm).

The calculated theoretical values of ARW for each optical head for four FORS type FOS6 were in the range of **4.49-4.85 nrad/s√Hz**, depending on total optical losses and fiber length in the given optical head.

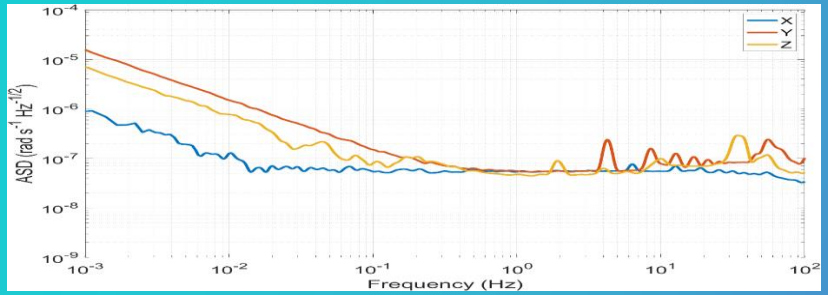

Allan Variance analysis
Data gathered in the Military University of Technology, Poland as Autonomous Rgresion Metod for Allan Variance (ARMAV) [Jurando, et al., *Navigation*, 66 (2019), 1-13]

ADEV(t)=√AVAR(t) ➔ ASD instead of PDS

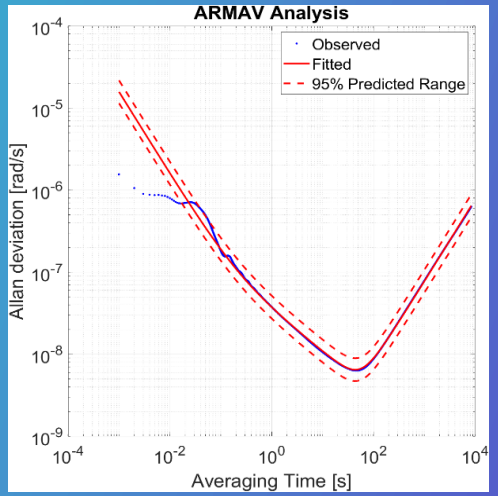

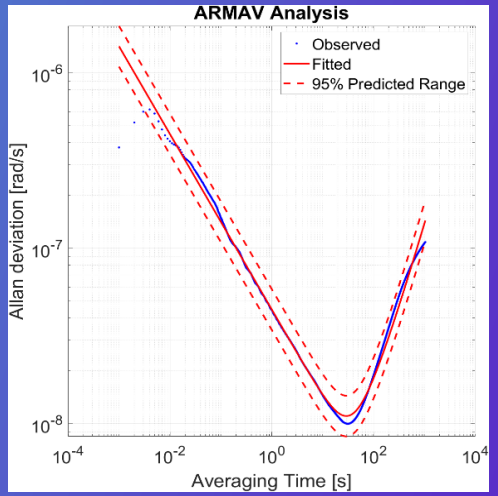

FOS6-01: ARW: 35 nrad/s/√Hz, BI: 10.0 nrad/s
FOS6-02: ARW: 45 nrad/s/√Hz, BI: 15.0 nrad/s

Correlation verification

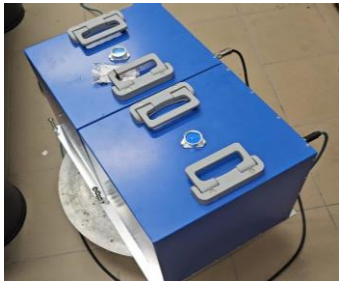

FOS6-01 and FOS6-02 in the MUT laboratory on the rotary table

Field test in the Kampinos Nature Park by a pair of FORSs (FOS6-01 and FOS6-04)

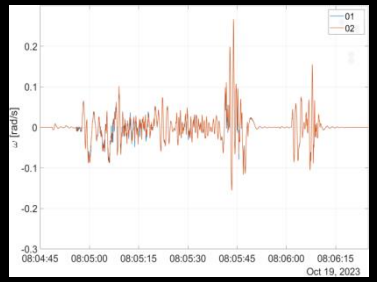

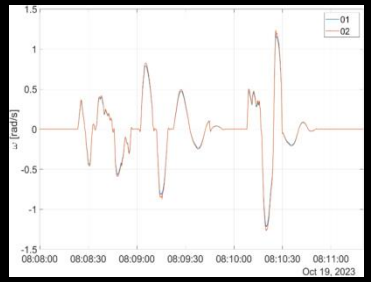

Signals recorded by FORSs Z-axes during the medium high-amplitude and fast-changing excitations as well as high-amplitude amplitude excitations

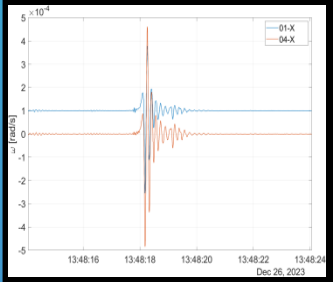

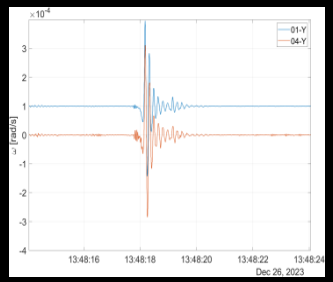

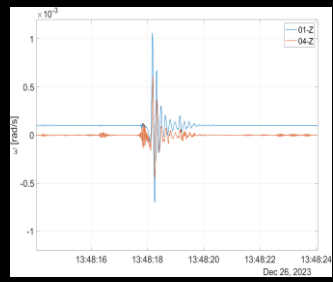

A weak rotational disturbance recording (with an amplitude of about 0.5 mrad/s) generated by the wild animal (elk) moving in the field close to the FORSs location

Pearson correlation coefficient equal to 99.42% and 99.99 %

Pearson correlation of about 95% for the X axis, about 99% for Y axis, and about 99% for the Z axis

ROTATION DETECTION DURING DETONATION OF AN EXPLOSIVE CHARGE

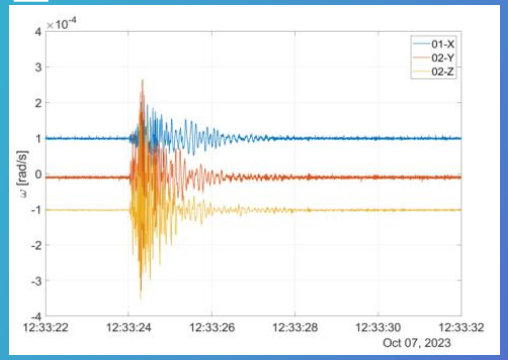

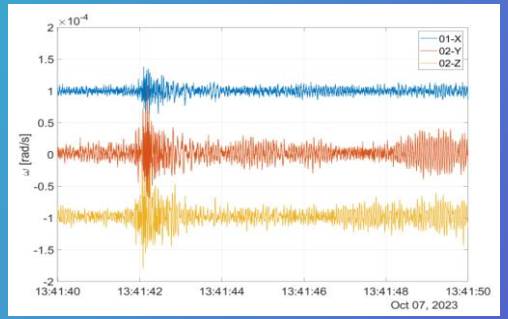

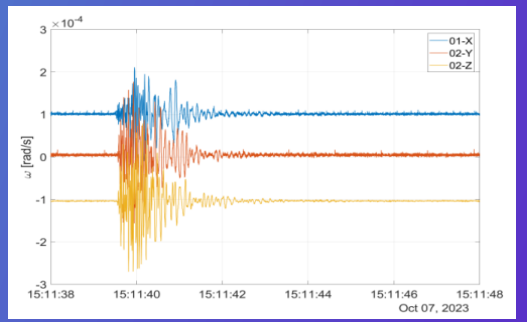

On the 7th of October 2023 there were three explosions performed:
1. 12:33 UTC, 5 kg of explosive, 3 m below the ground surface with surface discharge.
2. 13:41 UTC, 5 kg of explosive, 4.5 m below the ground surface without surface discharge.
3. 15:11 UTC, two 5 kg explosive charges installed 5 meters apart were detonated one after the other, 4.5 m below the ground surface, with a distance of 5 m between loads.

	A_{max} [μrad/s]			E_f [μrad]		
Explosion number/ Axis of FORS	X	Y	Z	X	Y	Z
Explosion 1	140	327	281	69	163	104
Explosion 2	38	108	83	41	98	94
Explosion 3	119	177	170	65	111	106

System control

Paramters change

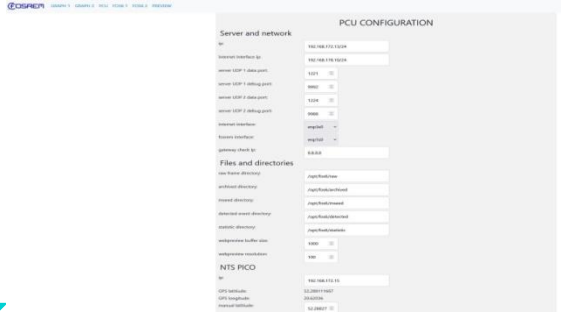

Data downloading

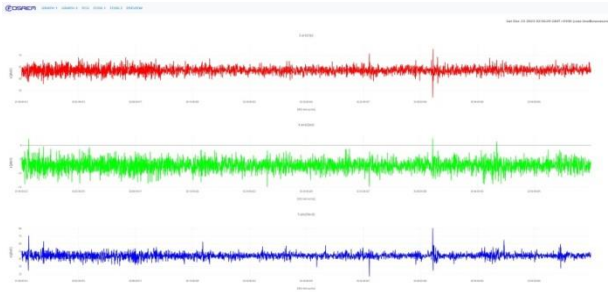

Localization

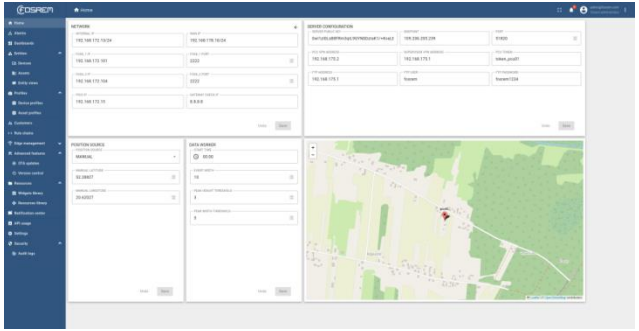

Remote control by webpage

Conclusions

1. Data confirmed high reliability of recordings gathered by 3-axial Fibre-Optic Rotational Seismograph (correlation coefficient was near the value of 100%)

2. FORS recorded successfully artificial explosions in field test carried out in Szopowe, Poland which confirmed its usefulness of monitoring detonation tests, especially in border areas.

3. FORS main paramters:
   - dynamics of 180 dB
   - frequency detection bandpass: from 0.01 to 100 Hz
   - built-in time scale synchronization system (accuracy 100ns)
   - weight: less than 10 kg
   - web-Based Management Interface
   - possibility of mobile, autonomous operation

4. Future plans – 6 DoF recordings

THANK YOU

ELPROMA ELECTRONICS

WAT

FOSREM - FROM SKY ACROSS GROUND UP TO UNDERGROUND

National Centre for Research and Development project POIR.01.01.01-00-1553/20-00

FOM-MEM - FIBRE-OPTIC MATRIX FOR MECHANICAL EVENTS MAPPING

Polish Agency for Enterprise Development project FENG.01.01-IP.02-1714/23

Fundusze Europejskie dla Nowoczesnej Gospodarki

Rzeczpospolita Polska

Dofinansowane przez Unię Europejską

PARP Grupa PFR